Cortical Shape Analysis using the Anisotropic Global Point Signature

Anand A Joshi[1,3], Syed Ashrafulla[1], David W Shattuck[2], Hanna Damasio[3] and Richard M Leahy[1] *

[1] Signal and Image Processing Institute, University of Southern California, Los Angeles, CA
[2] Laboratory of Neuro Imaging, University of California, Los Angeles, CA
[3] Brain and Creativity Institute, University of Southern California, Los Angeles, CA

Abstract. We present a novel shape representation that characterizes the shape of a surface in terms of a coordinate system based on the eigensystem of the anisotropic Laplace-Beltrami operator. In contrast to the existing techniques, our representation can capture developable transformations and is therefore useful for analysis of cortical folding patterns. This representation has desirable properties including stability, uniqueness and invariance to scaling as well as isometric transformations. Additionally, the resulting shape space has a standard Euclidean metric simplifying shape analysis. We also present an approach that provides a fast and accurate computational method for solving the eigensystem using a finite element formulation. We demonstrate the utility of this representation for two brain shape analysis applications: quantifying symmetries in shape between the two cortical hemispheres and finding variance of cortical surface shapes across populations.

1 Introduction

Quantification, matching and comparison of cortical shapes are challenging problems with wide utility [17,12]. Most of the traditional approaches for analyzing brain shapes are deformation-based. Quantitative analysis of anatomical shape differences is performed with these approaches by analyzing the deformation required to warp a subject brain to a template brain. For example, tensor-based morphometry [8] analyzes local linear approximations (the deformation tensors) of the deformation field. Alternate methods such as deformation-based morphometry [1] and pattern-based morphometry [3] use different aspects of the deformation field.

While quantification of shape differences by analysis of the deformation field is a plausible approach, it suffers from a number of disadvantages. The results of these methods depend to a large extent on the image registration method used. Only regions where registration works well – typically subcortical structures – tend to show high statistical power [8]. Using the deformation field as a shape

* This work was supported by NIH grants P41 EB015922 and R01 NS074980.

descriptor often magnifies the effects of registration errors. In addition, it is not clear if the shape details are indeed encoded in the deformation tensor as this tensor is a local linear approximation of the deformation field. This is especially the case for large shape differences that require large deformations. Also, there is no ground truth deformation for the purpose of aligning one brain to another; in other words, registration may provide only one of multiple equally accurate deformation fields from one brain image to another. Finally, the deformation field does not define a shape space on the cortex in the sense that sulcal and gyral shapes are not directly encoded in the deformation field.

Recent approaches for brain shape analysis are based on spectral geometry, in which the shape of a manifold is characterized by the eigenspectrum of a differential operator defined on the manifold. An invariant representation of a 2D surface can be generated using the Global Point Signature (GPS) representation, which is based on the eigensystem of the isotropic Laplace-Beltrami operator defined on that surface [13,14]. Methods using GPS are not directly applicable

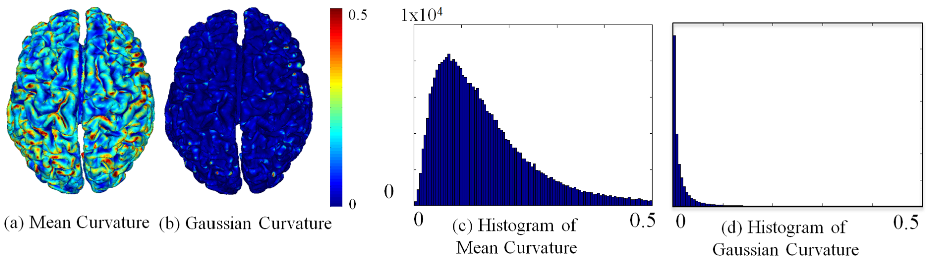

Fig. 1. Absolute value of mean and Gaussian curvature of a cortical surface.

to cortical shape analysis because the isotropic Laplace-Beltrami operator only captures the intrinsic geometry of the surface. The majority of the curvature information of the cortex is in the mean curvature, as seen in figure 1, which is extrinsic to the surface. 3D shape descriptors such as spherical harmonics [7] are not convenient for cortical shape analysis since such descriptors require an impractically large number of basis functions and do not efficiently encode shape information related to elastic deformations of shapes. This paper presents an approach for shape analysis of 2D surface patches using an anisotropic version of the Laplace-Beltrami operator as described in the next section.

2 Materials and Methods

2.1 AGPS Shape Representation

We assume as input an anatomically labeled cortical surface representation such as obtained by BrainSuite [15,6]. Motivated by spectral theory [14,13,5], we model a surface S representing a cortical region as an inhomogeneous vibrating membrane. Its harmonic behavior is thus governed by the 2D anisotropic

Helmholtz equation where the mean curvature $\kappa(s)$ is used to introduce anisotropy:

$$\begin{cases} \nabla \cdot \kappa(s)\nabla\Phi(s) & = \lambda\Phi(s) \\ \frac{\partial\Phi(s)}{\partial \boldsymbol{n}}|_{\partial S} & = 0 \end{cases}, \forall s \in S, \tag{1}$$

where ∇ denotes a gradient operator defined in the geometry of the surface, $\Phi(s)$ represents an eigenfunction with eigenvalue λ, ∂S is the boundary of the surface patch and $\boldsymbol{n}$ is the normal to the surface. We use the eigenfunctions and eigenvalues to define the Anisotropic Global Point Signature (AGPS) embedding of the surface S in the spectral domain by the map:

$$\mathrm{AGPS}(s) = \left(\frac{1}{\sqrt{\lambda_1}}\Phi_1(s), \frac{1}{\sqrt{\lambda_2}}\Phi_2(s), \frac{1}{\sqrt{\lambda_3}}\Phi_3(s), \ldots\right), \, p \in S \tag{2}$$

where $\Phi_1, \Phi_2, \ldots$ are eigenfunctions with corresponding eigenvalues $\lambda_1, \lambda_2, \ldots$ arranged in ascending order. Thus, each point of the manifold is embedded into an infinite-dimensional space. The importance of modeling anisotropy in the representation is illustrated in figure 2. A developable transformation (bending)

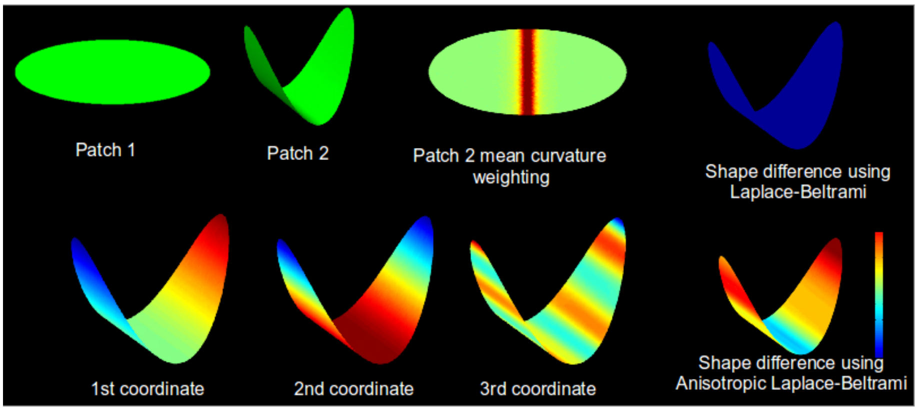

Fig. 2. Introduction of an anisotropic term helps characterize developable transformations. Use of the isotropic Laplace-Beltrami operator does not find any shape differences between the two elliptical patches as the transformation between the two is developable (top right). Use of an anisotropic operator with a mean curvature anisotropy helps in capturing the shape differences (bottom right). The resulting AGPS coordinates are also shown in the bottom row.

applied to an elliptical surface does not affect the intrinsic geometry of the surface and therefore the Gaussian curvature remains unchanged. However, the extrinsic geometry is altered by this transformation resulting in changes in mean curvature. It can be seen that the bending does not change the isotropic Laplace-Beltrami eigenspectrum and therefore the shape change is not detected by GPS. However, the anisotropy introduced via the mean curvature allows the AGPS to successfully capture the change in the shape.

The AGPS embedding presented in equation (2) has many favorable properties. First, its coordinates are isometry invariant as they depend only on the derivatives and curvature, which in turn are dependent only on the shape. Second, scaling the manifold by a factor α results only in scaling mean curvature by $1/\alpha$. Therefore, we can obtain scale-invariance if desired by normalizing the eigenvalues; however, for the specific application of cortical shape representation, we do not want scale-invariance. Third, changes of the manifold's shape result in continuous changes in the spectrum so the representation is stable. Fourth, in the embedding space, the inner product is given by the anisotropic Green's function due to the identity $G(s_1, s_2) = \sum_k \frac{\Phi_k(s_1)\Phi_k(s_2)}{\lambda_k}$, $s_1, s_2 \in S$ [13]. As a result, the AGPS representation encodes anisotropic diffusion distances [9] on the surface. In addition, both local and global shape information is represented in the embedding. Finally, in this infinite-dimensional shape space, the metric is Euclidean, allowing standard ℓ^2 space analysis.

This invariant spectral geometric representation of surfaces has interesting physical interpretations. The surfaces can be modeled as vibrating membranes and the vibrations are damped proportionally to the mean curvature at each point. The anisotropic Laplace-Beltrami eigenspectrum corresponds to the modes of vibrations of this membrane (Fig. 2 (bottom)). Thus the AGPS representation encodes information about the modes of vibration of membranes (surface patches) as the basis for shape modeling. The AGPS shape representation intuitively encodes curvature characteristic at and around the points on the manifold. Perturbations at a point in a shape lead to local changes in curvature around that point which are captured in higher-order AGPS coordinates. On the other hand global shape changes lead to curvature changes everywhere in the shape which are captured by lower-order AGPS coordinates. Due to this association between AGPS coordinates and the spatial extent of shape changes, AGPS-based comparisons provide a natural description of changes in shape at different scales.

2.2 Numerical Implementation

To solve equation (1) we first compute the anisotropy term represented by mean curvature using the method described in [10]. Next, we use a finite element method (FEM) to discretize the anisotropic Helmholtz equation (1). We discretize the derivative operators using FEM directly in the geometry of the surface mesh, and therefore we do not need to explicitly compute the Riemannian metric coefficients as is often done if the surfaces are mapped to a plane or sphere [17]. We choose linear FEMs for functions and Galerkin's formulation [16] for robustness to tessellation errors. Let $\Phi(s) = \sum_i \phi_i e_i(s)$ be an eigenfunction and $N(s) = \sum_i \eta_i e_i(s)$ be a 'test function', each represented as weighted sums of linear elements $e_i(s)$. The eigenvalue problem from equation (1) then becomes:

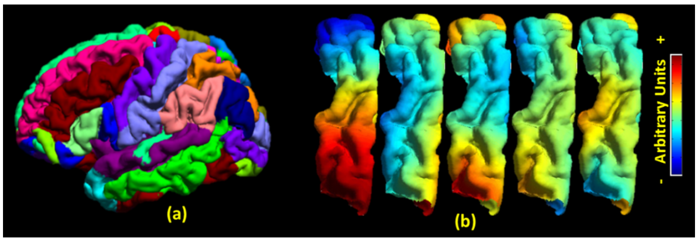

Fig. 3. An AGPS example: (a) automatically generated parcellations of a cortical surface; (b) first five color-coded AGPS coordinates of the left superior-frontal gyrus.

$$\begin{aligned} (\nabla \cdot \kappa(s) \nabla)\, \Phi(s) =& \lambda \Phi(s) \\ \implies \int_S (\nabla \cdot \kappa(s) \nabla \Phi(s))\, N(s) ds =& \lambda \int_S \Phi(s) N(s) ds \\ \implies -\int_S \kappa(s) \nabla \Phi(s) \nabla \eta N(s) ds =& \lambda \int_S \Phi(s) N(s) ds \end{aligned}$$

where the latter follows using integration by parts and Neumann boundary conditions in equation (1). Substituting the FEM into this equation, we get:

$$\begin{aligned} -\sum_i \sum_j \phi_i \eta_j \kappa_{ij} \int \nabla e_i(s) \nabla e_j(s) ds =& \lambda \sum_i \sum_j \phi_i \eta_j \int e_i(s) e_j(s) ds \\ \implies KS\Phi =& -\lambda M \Phi \end{aligned} \quad (3)$$

where $\kappa_{ij} = \frac{\kappa_i + \kappa_j}{2}$ is the average of curvatures calculated at points i and j, K is a matrix with i^{th} row and j^{th} column given by κ_{ij}, and Φ is a column vector with i^{th} entry given by ϕ_i. For a triangulated surface mesh with linear elements, the element-wise matrix is given by $M_{el} = \frac{A_{el}}{12} \begin{bmatrix} 2 & 1 & 1 \\ 1 & 2 & 1 \\ 1 & 1 & 2 \end{bmatrix}$ and the element-wise stiffness matrix is given by $S_{el} = D_x D_x + D_y D_y$ where D_x and D_y are discretizations of derivatives in the x and y directions, respectively. The mass and stiffness matrices M and S are obtained from the corresponding element-wise matrices M_{el} and S_{el} respectively by finite element matrix assembly procedures as described in [16]. The matrix equation (3) is a generalized eigenvalue problem that can be solved using standard methods such as the QZ method in the Matlab function `eigs`. For this analysis, we chose to approximate the infinite-dimensional AGPS by its first seven coordinates based on the spread of the eigenvalue spectrum. One example of the computed AGPS coordinates for the surface patch representing the left superior frontal gyrus is shown in figure 3.

2.3 Brain Shape Analysis using AGPS

In order to illustrate the potential of the proposed representation for cortical shape analysis, we apply AGPS for two group studies of $N = 24$ subjects: (1)

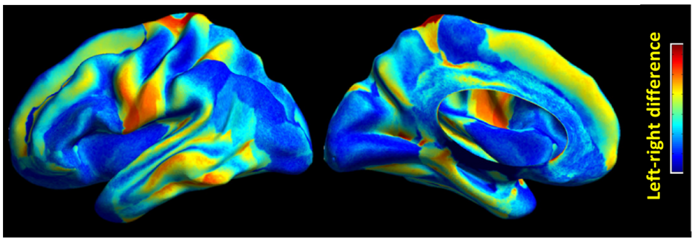

Fig. 4. Left-to-right hemisphere average shape difference, based on gyral AGPS. The color-coded overlay shows the degree of symmetry (blue) and asymmetry (red).

asymmetry analysis and (2) variability analysis. For this purpose, we generated the AGPS coordinates for each vertex using the method described in the previous section. While it is possible to get a full description of shape change at different scales by analyzing coordinate-wise AGPS differences, we summarize the shape difference with ℓ^2-norm since the shape space admits an Euclidean metric.

To map symmetry between the left and right hemispheres of subjects, we first define AGPS_L and AGPS_R as the AGPS representations of left and right cortical hemispheres of a subject and transfer them to the common atlas space for comparison. We register the atlas's right hemisphere R to the atlas's left hemisphere L forming a correspondence denoted by $\Psi : R \to L$. With this correspondence, we can then compute mean AGPS distance between hemispheres at each vertex s in the atlas's right hemisphere by $D(s) = \|\mathrm{AGPS}_L(\Psi(s)) - \mathrm{AGPS}_R(s)\|_2$. To find group asymmetry, we average $D(s)$ over all the subjects.

Shape variability on the cortex can be found by estimating the population variance of the AGPS coordinates. We compute the AGPS coordinates for each subject in the native space and then transfer these coordinates to the standard atlas space. We then estimate the population variance at each vertex s in the atlas space by $\sigma^2(s) = \frac{1}{N}\sum_{n=1}^{N}\left(\mathrm{AGPS}_n(s) - \frac{1}{N}\sum_{m=1}^{N}\mathrm{AGPS}_m(s)\right)^2$. Note that we use the correspondence established using surface registration for comparing the shapes in the atlas domain, but we do not use the deformation field as a shape descriptor due to the reasons discussed in section 1.

3 Results

3.1 Asymmetry across hemispheres

After parcellation, the left and right hemispheres of a subject's brain contain homologous regions that may differ in shape. This hemispheric brain asymmetry is possibly related to functional lateralization due to evolutionary, hereditary and developmental factors [18]. In order to map cortical asymmetry, we use the procedure described in section 2.3 with results shown in figure 4. The most asymmetric regions are in the inferior sector of the pre- and post-central gyrus, the mid portion of the middle temporal gyrus and posterior portion of the inferior temporal gyrus, and, to a lesser extent in the mesial sector of the superior frontal

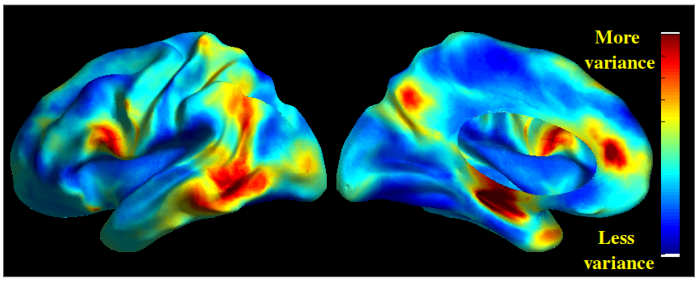

Fig. 5. Population variance of cortical shape. The color-coded overlay is the variance of the AGPS representation, plotted on an inflated representation of the cortex.

gyrus. One slightly surprising result is that there is minimal asymmetry at the end of the Sylvian fissure and needs further investigation.

3.2 Variability in Shapes

In addition to analyzing shape variability between cortical hemispheres across the subject population, we can analyze the variability in cortical shape over a population. In figure 5 on the left (lateral aspect of the hemisphere) we see high variability in the posterior sector of the middle and inferior temporal gyri and the inferior parietal lobule hugging the posterior end of the Sylvian fissure, as well as in the frontal operculum; on the right (mesial aspect of the hemisphere) the areas of maximal variability are found in the pre-cuneus, the anterior sector of the cingulate gyrus and in the anterior sector of the parahippocampal gyrus (site of the maximal variance). Most of these regions are in the association cortex.

4 Discussion and Conclusion

This paper presents a new invariant shape representation, AGPS, that captures differences in surface shapes due to developable transformations, a critical class of transformations in the analysis of cortical folds. The shape space generated by this representation is ℓ^2, readily allowing the use of existing standard statistical techniques for shape analysis. We illustrated the benefits of AGPS in quantifying shape differences across hemispheres and shape variation across subjects.

The question of whether a surface is unique (within an isometry) given its AGPS coordinates is related to the existence of Bonnet surfaces, i.e. surfaces that are not completely defined by their metric and mean curvature [2]. However, it is unlikely that cortical surfaces would suffer from such an ambiguity. Another possible ambiguity is in the order of eigenfunctions of the anisotropic Laplace-Beltrami operator in cases where there are repeated eigenvalues, which can occur if there are certain symmetries in the shape. An algorithm for resolving this ambiguity can be found in [4]. For the purpose of brain shape analysis, we did not encounter any ambiguity possibly due to shapes not having axes of symmetry.

Many aspects of the preprocessing can affect the AGPS representations of cortical regions, thus introducing sources of error in cortical shape analysis.

More specifically, it is unclear whether different parcellation schemes can result in different shape analysis results. We note that recent registration and labeling methods can parcellate the brain with accuracy approaching manual labeling [11]. In the future, we plan to explore the effect of parcellation decisions on cortical shape analysis using AGPS.

The presented AGPS representation and analysis methods can be applied for applications other than cortical shape analysis. AGPS representations can help in various computer vision applications requiring shape analysis where the intrinsic geometry does not fully capture the shape. In addition, this representation can also be extended to 3 or more dimensions using approaches presented in this paper for 2D surfaces and in previous work for 1D curves [5].

References

1. Ashburner, J., Hutton, C., Frackowiak, R., Johnsrude, I., Price, C., Friston, K.: Identifying global anatomical differences: deformation-based morphometry. Human Brain Mapping 6(5-6), 348–357 (1998)
2. Bobenko, A., Eitner, U.: Bonnet surfaces and Painlevé equations. Journal fur die Reine und Angewandte Mathematik 499, 47–80 (1998)
3. Gaonkar, B., Pohl, K., Davatzikos, C.: Pattern based morphometry. Proc MICCAI pp. 459–466 (2011)
4. Jain, V., Zhang, H.: Robust 3D shape correspondence in the spectral domain. In: SMI 2006. pp. 19–19. IEEE (2006)
5. Joshi, A., Ashrafulla, S., Shattuck, D., Damasio, H., Leahy, R.: An invariant shape representation using the anisotropic Helmholtz equation. MICCAI 2012 pp. 607–614 (2012)
6. Joshi, A., Shattuck, D., Leahy, R.: A method for automated cortical surface registration and labeling. In: Proceedings of the 5th international conference on Biomedical Image Registration. pp. 180–189. Springer-Verlag (2012)
7. Kazhdan, M., Funkhouser, T., Rusinkiewicz, S.: Rotation invariant spherical harmonic representation of 3D shape descriptors. In: Proc Eurographics/ACM SIGGRAPH. pp. 156–164. Eurographics Association (2003)
8. Lepore, N., Brun, C., Chou, Y., Chiang, M., Dutton, R., Hayashi, K., Luders, E., Lopez, O., Aizenstein, H., Toga, A., et al.: Generalized tensor-based morphometry of HIV/AIDS using multivariate statistics on deformation tensors. IEEE Trans Med Image 27(1), 129–141 (2008)
9. Lipman, Y., Rustamov, R., Funkhouser, T.: Biharmonic distance. ACM Transactions on Graphics (TOG) 29(3), 27 (2010)
10. Meyer, M., Desbrun, M., Schröder, P., Barr, A.: Discrete differential-geometry operators for triangulated 2-manifolds. Visualization and Math 3(7), 34–57 (2002)
11. Pantazis, D., Joshi, A., Jiang, J., Shattuck, D., Bernstein, L., Damasio, H., Leahy, R.: Comparison of landmark-based and automatic methods for cortical surface registration. NeuroImage 49(3), 2479–2493 (2010)
12. Rettmann, M.E., Prince, J.L., Resnick, S.M.: Analysis of sulcal shape changes associated with aging. Proc Human Brain Mapping (2003)
13. Reuter, M.: Hierarchical shape segmentation and registration via topological features of Laplace-Beltrami eigenfunctions. IJCV 89(2), 287–308 (Sep 2010)
14. Rustamov, R.: Laplace-Beltrami eigenfunctions for deformation invariant shape representation. In: Proc 5th Euro Symp Geom Proc. pp. 225–233 (2007)

15. Shattuck, D.W., Leahy, R.M.: BrainSuite: An automated cortical surface identification tool. Medical Image Analysis 8(2), 129–142 (2002)
16. Smith, G.D.: Numerical solution of partial differential equations: Finite difference methods. Oxford : Clarendon Press (1985)
17. Thompson, P., Woods, R., Mega, M., Toga, A.: Mathematical/computational challenges in creating deformable and probabilistic atlases of the human brain. Human Brain Mapping 9(2), 81–92 (2000)
18. Toga, A., Thompson, P.: Mapping brain asymmetry. Nature Reviews Neuroscience 4(1), 37–48 (2003)